

LETTER

Optimal temperature for malaria transmission is dramatically lower than previously predicted

Erin A. Mordecai,^{1,*} Krijn P. Paaijmans,² Leah R. Johnson,³ Christian Balzer,^{1,†} Tal Ben-Horin,⁴ Emilyde Moor,⁵ Amy McNally,⁵ Samraat Pawar,⁶ Sadie J. Ryan,⁷ Thomas C. Smith¹ and Kevin D. Lafferty^{1,8}

Abstract

The ecology of mosquito vectors and malaria parasites affect the incidence, seasonal transmission and geographical range of malaria. Most malaria models to date assume constant or linear responses of mosquito and parasite life-history traits to temperature, predicting optimal transmission at 31 °C. These models are at odds with field observations of transmission dating back nearly a century. We build a model with more realistic ecological assumptions about the thermal physiology of insects. Our model, which includes empirically derived nonlinear thermal responses, predicts optimal malaria transmission at 25 °C (6 °C lower than previous models). Moreover, the model predicts that transmission decreases dramatically at temperatures > 28 °C, altering predictions about how climate change will affect malaria. A large data set on malaria transmission risk in Africa validates both the 25 °C optimum and the decline above 28 °C. Using these more accurate nonlinear thermal-response models will aid in understanding the effects of current and future temperature regimes on disease transmission.

Keywords

Anopheles, climate change, disease ecology, malaria, *Plasmodium falciparum*, temperature.

Ecology Letters (2013) 16: 22–30

INTRODUCTION

Malaria presents a substantial public health and financial burden (WHO 2011). In 2010 alone, there were an estimated 216 million cases worldwide and at least 655 000 deaths, with most morbidity and mortality occurring in sub-Saharan Africa (WHO 2011). An estimated US\$ 2 billion was spent on malaria control in 2011 (WHO 2011). Despite the enormous global burden of malaria, after more than a century of research we still have a poor understanding of the mechanistic link between environmental variables, such as temperature and malaria risk (Lafferty 2009; Paaijmans *et al.* 2009; Pascual *et al.* 2009). Temperature is fundamentally linked to malaria mosquito and parasite vital rates, and understanding the role of temperature in malaria transmission is particularly important in light of climate change. The goal of this article is to determine how environmental temperature drives malaria transmission via its combined effects on the mosquito and parasite vital rates that determine transmission. By determining the temperature sensitivity of malaria transmission, we can then apply our model to understand both the effect of current ambient conditions and the potential effect of future changes in temperature on malaria transmission.

A key epidemiological metric for understanding malaria risk is the Basic Reproductive Number (R_0), which defines the number of cases of a disease that arise from one case introduced into a popula-

tion of susceptible hosts. Epidemics can proceed only if R_0 exceeds one, and disease prevalence increases with R_0 . This transmission metric depends on mosquito density, biting rate, vector competence and survival rate as well as parasite development time within the mosquito (i.e. extrinsic incubation time) and human recovery rate. Mosquito density is in turn a function of adult survival and fecundity, and immature development time and survival (see Appendix S1 in the Supporting Information; Table 2).

Given that all of these parameters except human recovery rate relate to mosquito abundance, biology or physiology, and that mosquitoes are small cold-blooded insects, it is clear that environmental temperature will influence the transmission intensity of malaria (Craig *et al.* 1999; Rogers & Randolph 2006; Parham & Michael 2010). Existing malaria risk models that factor in effects of climate (Martens *et al.* 1997; Craig *et al.* 1999; Hoshen & Morse 2005; Parham & Michael 2010; Alonso *et al.* 2011; Ermert *et al.* 2011; Gething *et al.* 2011) have used monotonically increasing relationships between temperature and mosquito and parasite vital rates. Other variables are assumed to be temperature insensitive (see Table 1).

In reality, ectotherm performance measures, such as development rate, survival probability and reproductive rate, increase from zero at a critical minimum temperature (CT_{min}), peak at an optimum temperature (T_{opt}), then sharply decline to zero at a critical maximum temperature (CT_{max} ; Angilletta 2009; Dell *et al.* 2011). These unimo-

¹Ecology, Evolution, and Marine Biology Department, University of California, Santa Barbara, CA, 93106, USA

²Center for Infectious Disease Dynamics, Department of Entomology, Penn State University, Merkle Lab, University Park, PA, 16802, USA

³Department of Ecology and Evolution, University of Chicago, 1101 E 57th Street, Chicago, IL, 60637, USA

⁴Bren School of Environmental Science and Management, University of California, Santa Barbara, CA, 93106, USA

⁵Geography Department, University of California, Santa Barbara, CA, 93106, USA

⁶Department of Biomathematics, David Geffen School of Medicine, University of California, Los Angeles, CA, 90095-1766, USA

⁷Department of Environmental and Forest Biology and Division of Environmental Science, College of Environmental Science and Forestry, State University of New York, 1 Forestry Drive, Syracuse, NY, 13210, USA

⁸Western Ecological Research Center, U.S. Geological Survey, Marine Science Institute, University of California, Santa Barbara, CA, 93106, USA

*Correspondence: E-mail: Mordecai@lifesci.ucsb.edu

†Deceased.

Table 1 Comparing the temperature ranges of the new model to previous mechanistic malaria transmission models. The model, predicted minimum, maximum and optimum temperatures, and the functional forms for all temperature-sensitive parameters are listed. This list is restricted to the mechanistic (as opposed to statistical) malaria models that provide optimal temperature estimates. Many other models use linear thermal responses, but do not provide optimal temperatures, and so are not directly comparable with our model

Model	Min. (°C)	Max. (°C)	Opt. (°C)	Transmission metric
This paper	17	34	25	R_0
Parham & Michael (2010)	20	39	32–33	R_0
Craig <i>et al.</i> (1999)	18	40	30	p^{EIP} (fraction of vectors surviving sporogony)
Martens <i>et al.</i> (1997)	18	38	31	Epidemic potential (reciprocal of the critical mosquito density necessary to maintain parasite transmission)

Temperature-dependent parameters and functional forms	
Quadratic:	vector competence, proportion of eggs that produce adults, daily adult survival, eggs per female per day
Briere:	parasite development rate, mosquito development rate, biting rate
Linear (or combination of linear functions):	total number of mosquitoes, biting rate, proportion of infected mosquitoes that become infectious
Unimodal:	adult mortality rate
Linear:	parasite development time within the mosquito, larval duration
Nonlinear monotonic:	adult daily survival probability
Linear:	parasite development time within the mosquito, biting rate
Unimodal:	adult daily survival probability

dal temperature responses are used for a wide range of ecological and evolutionary applications (Huey & Berrigan 2001; Amarasekare & Savage 2012), including the effects of climate change on ectotherms (Deutsch *et al.* 2008; Neuheimer *et al.* 2011). Such relationships have been established for several malaria mosquito and parasite life-history traits, including immature development and survival (Lyimo *et al.* 1992; Bayoh & Lindsay 2003), gonotrophic cycle length (Lardeux *et al.* 2008) and parasite development times (Ikemoto 2008; Paaijmans *et al.* 2009). However, most models of R_0 or other transmission metrics for vector-borne diseases such as malaria use linear or monotonic thermal responses, putting the accuracy of existing models into question (Table 1; Martens *et al.* 1997; Craig *et al.* 1999; Parham & Michael 2010).

Here, we fit unimodal temperature responses to all mosquito and parasite life-history traits that shape R_0 , using published data from laboratory studies of *Anopheles* mosquito species and *Plasmodium falciparum* malaria parasites conducted across a range of constant temperatures (Table 2). Although there is a wealth of field data on how mosquito (e.g. Bodker *et al.* 2003) and parasite (e.g. Afrane *et al.* 2007) traits vary in the field, mechanistic models of responses to temperature need to separate the effect of temperature from other variables such as differences in temperature variability, humidity, household occupancy and household practices between the studied areas. In addition, to build such models, responses to constant temperature are needed, repeated across a range of temperatures. Such data were available for many traits. However, in some cases, we had to approximate responses from other species, prompting us to determine the sensitivity of our results to these parameters (see Materials and Methods). We combined these novel temperature–life history relationships to derive the relationship between malaria transmission (R_0) and temperature.

We validated the model using an independently published data set. Our proxy for R_0 was the Entomological Inoculation Rate (EIR) from Africa (1979–1996). EIR is the rate at which people are bitten by infectious mosquitoes and is a combination of several mosquito and parasite life-history traits, including parasite extrinsic incubation period (EIP), vector competence, mosquito survival and biting rate (Smith *et al.* 2007). We plotted EIR against mean temperature during the transmission season and compared the shape of this observed relationship with estimates from our model.

MATERIALS AND METHODS

Data collection

We collected data on mosquito and parasite vital rates from laboratory studies that measured *Anopheles* spp. mosquitoes and *P. falciparum* parasites at a range of constant temperatures (Table 2). Laboratory studies with constant temperatures were required to isolate the effect of temperature and remove confounding variables such as variation in temperature and humidity. Although daily temperature variation is important for transmission, it can be incorporated by integrating our model over a realistic temperature regime (Paaijmans *et al.* 2009, 2010), and this work is currently in progress. We recorded data by hand or digitised figures using DigitizerIt (Borland 2001–2010) and Engauge (GNU General Public License, digitizer.sourceforge.net) software. We derived mortality rate data from time series of mosquito survival over time, as described in Appendix S1. Although Bayoh & Lindsay (2003) data used for mosquito development rate

Table 2 The relationships between temperature and the mosquito and parasite life-history traits that determine malaria risk. For each variable, the species studied and the source(s) of the data are given. Thermal performance curves were fitted to the data assuming Briere $cT(T - T_0)(T_m - T)^{1/2}$, B, or Quadratic $[qT^2 + rT + s]$ functions, Q, in which T is temperature (°C; see Materials and Methods). Standard deviations for the model parameters are listed in parentheses alongside parameter values. Best fit was determined by Akaike Information Criterion (AIC). The data and best-fit model for each parameter are plotted in Fig. 1

Parameter	Definition	Species	Source	Fit	Fit parameters (standard deviation)
a	Biting rate (mean oviposition time) ⁻¹	<i>Anopheles pseudopunctipennis</i>	Lardeux et al. (2008)	B	$c = 0.000203$ (0.0000576) $T_m = 42.3$ (3.53) $T_0 = 11.7$ (2.47)
b^*c	Vector competence	<i>Anopheles quadrimaculatus</i>	Stratman-Thomas (1940)	Q	$q = -0.54$ (0.18) $r = 25.2$ (9.04) $s = -206$ (108)
p [$p = e^{-\mu}$]	Daily adult survival probability (ϕ); adult mortality rate (μ)	<i>Anopheles gambiae</i>	Bayoh (2001)	Q	$q = -0.000828$ (0.0000519) $r = 0.0367$ (0.00239) $s = 0.522$ (0.0235)
PDR	Parasite development rate (PDR); extrinsic incubation period (EIP)	<i>An. gambiae</i> , <i>Anopheles culicifacies</i> , <i>Anopheles stephensi</i> , <i>An. quadrimaculatus</i> , <i>Anopheles atroparvus</i>	Boyd & Stratman-Thomas (1933); Knowles & Basu (1943); Siddons (1944); Shute & Maryon (1952); Vaughan et al. (1992); Eling et al. (2001)	B	$c = 0.000111$ (0.0000161) $T_m = 34.4$ (0.000176) $T_0 = 14.7$ (1.48)
p_{EA}	Egg-to-adult survival probability	<i>An. gambiae</i>	Bayoh & Lindsay (2003)	Q	$q = -0.00924$ (0.00123) $r = 0.453$ (0.0618) $s = -4.77$ (0.746)
MDR	Mosquito development rate (MDR); larval development time (τ_{EA})	<i>An. gambiae</i>	Bayoh & Lindsay (2003)	B	$c = 0.000111$ (0.00000954) $T_m = 34$ (0.000106) $T_0 = 14.7$ (0.831)
EFD	Eggs laid per adult female per day	<i>Aedes albopictus</i>	Delatte et al. (2009)	Q	$q = -0.153$ (0.0307) $r = 8.61$ (1.69) $s = -97.7$ (22.6)

(MDR) and egg-to-adult survival give water temperatures, rather than air temperatures, the experiments were carried out in climate chambers, so water temperatures should be similar to air temperatures.

We made exceptions to our standards for data inclusion in two instances. No reliable *Anopheles* spp. fecundity data at controlled temperatures were available, so we used data from the tropical species *Aedes albopictus*. Although using temperature-sensitive fecundity data from a different genus of mosquitoes is not ideal, these were the best available data with which to estimate this relationship. Two laboratory *Anopheles gambiae* fecundity studies conducted at 27 °C indirectly suggest that the *A. albopictus* fecundity data were appropriate for our predictions (Takken et al. 1998, 2002). Egg production was high in these studies, indicating that 27 °C was an ideal temperature for egg production and suggesting that it is near the optimum for *A. gambiae*. Because we found that the peak fecundity for *A. albopictus* was at 28 °C, we can assume that the temperature–fecundity response of the two species overlap considerably. This, along with the insensitivity of our results to variation in the temperature for peak fecundity adds more confidence to this critical assumption. Shifting the fecundity peak by 3 °C would only shift the R_0 peak by 0.3 °C (see Results for further sensitivity analysis). In addition to fecundity, vector competence data for *Anopheles* mosquitoes with *P. falciparum* were not available, so we used *Anopheles* with *Plasmodium vivax*. Although *P. vivax* can tolerate cooler temperatures than *P. falciparum*, the vector competence data were similar to results from a poorly controlled *P. falciparum* study (Siddons 1944), suggesting that vector competence is a mosquito trait. Regardless, increasing the vector competence peak by 3 °C would only shift the R_0 peak by 0.2 °C (see Results for further sensitivity analysis); therefore the use of *P. vivax* vector competence data was unlikely to affect the model outcome.

Fitting thermal-response models

Theory and data concur that biological rates typically show unimodal responses to temperature because underlying biochemical processes change irreversibly with temperature (Johnson et al. 1974). Metabolic reaction rates tend to increase exponentially up to an optimal temperature, then decline due to protein degradation and other processes (Johnson et al. 1974; Dell et al. 2011). Because the decline often occurs more rapidly than the rise, unimodal temperature responses are often left skewed (Dell et al. 2011; Englund et al. 2011). Two recent meta-analyses on the response of biological traits to temperature, including life-history parameters in insects, support these generalities (Dell et al. 2011; Englund et al. 2011). As all rate parameters in the temperature-dependent R_0 model are expected to be unimodal with respect to temperature, we fit quadratic and Briere functions (Briere et al. 1999) to each life-history parameter, as well as a linear function for comparison (Table S1). The Briere function is a left-skewed unimodal curve with three parameters, which represent the minimum temperature, maximum temperature and a rate constant (Briere et al. 1999). The unimodal functions are defined as Briere $[cT(T - T_0)(T_m - T)^{1/2}]$ and quadratic $[qT^2 + rT + s]$, where T is temperature in degrees Celsius and c , T_0 and T_m and q , r and s are fit parameters of each function respectively [Correction added on 5 November 2012, after first online publication: $c(T_0 - T)(T_m - T)^{1/2}$ has been changed to $cT(T - T_0)(T_m - T)^{1/2}$ in the preceding sentence, and in the caption of Table 2].

We fit all models using nonlinear least squares, with the ‘nls’ function in R (R Core Development Team, version 2.10.0), which

converges on the ordinary least squares (OLS) fit for the quadratic and linear functions (Seber & Wild 2003). Where possible, we chose among the candidate models using Akaike Information Criterion corrected for small sample sizes (AICc; Table 1). For fecundity (EFD), there were only four data points, so we chose the quadratic function visually. More data would clarify the precise relationship between *Anopheles* spp. fecundity and temperature.

Temperature-sensitive R_0 model

To formulate a fully temperature-sensitive R_0 model for malaria, we started with the widely used formula (Dietz 1993),

$$R_0 = \left(\frac{Ma^2 bce^{-\mu EIP}}{Nr\mu} \right)^{1/2} \quad (1)$$

where M is mosquito density, a is the per-mosquito biting rate, bc is vector competence (the product of the proportion of the bites by infective mosquitoes that infect susceptible humans and the bites by susceptible mosquitoes on infectious humans that infect mosquitoes), μ is the adult mosquito mortality rate, EIP is the extrinsic incubation period of the malaria parasite in mosquitoes, N is human density and r is the rate at which infected humans recover and acquire immunity. Note that some have used the square of this formula to represent R_0 (Dietz 1993), but the choice of model formula does not affect the estimated maximum, minimum or optimum temperatures for transmission.

We assumed that all mosquito and parasite parameters are temperature sensitive and that N and r , which depend directly on human physiology, are independent of environmental temperature. For mosquito density, $M(T)$, we used a formula based on the population density model developed by Parham & Michael (2010; see Appendix S1 for derivation). We expressed all times as rates (Table 2). The full temperature-sensitive malaria R_0 model is

$$R_0(T) = \left(\frac{a(T)^2 bc(T) e^{-\mu(T)/PDR(T)} EFD(T) p_{EA}(T) MDR(T)}{Nr\mu^3(T)} \right)^{1/2} \quad (2)$$

where (T) denotes a temperature-sensitive parameter response fitted from the data, PDR is the parasite development rate, EFD is the number of eggs laid per female per day, p_{EA} is the probability that a mosquito egg survives to become an adult and MDR is the larval mosquito development rate. We parameterised this model using the data and functional forms described in Table 2.

The fully parameterised temperature-sensitive R_0 model is presented in Fig. 2 ('new estimate'). For comparison, we also plotted a curve using Parham & Michael's (2010) temperature-sensitivity assumptions ('previous estimate'). We chose this curve to represent the predictions of previous models (Table 1) because it has the most temperature-sensitive parameters and its peak is similar to the other models. For direct comparison, we used the square-root R_0 formula for both curves (squaring the formula does not change the location of the curves along the temperature axis).

Validating the model using field data

We checked the accuracy of our model predictions using a published data set on the rate at which people were bitten by infectious mosquitoes – the EIR – from 14 countries in Africa [Mapping

Malaria Risk in Africa (MARA), <http://www.mara.org.za/>] (Hay *et al.* 2000). We collated these EIR data with temperature and rainfall data from the ERA40 reanalysis project from the European Centre for Medium-Range Weather Forecast (Uppala *et al.* 2005). EIR, a measure of transmission intensity, is defined as the product of the number of vectors per host (m), the mosquito daily biting rate (a) and the proportion of mosquitoes with the parasite in their salivary glands (s , sporozoite index). We used EIR because extensive data on R_0 in the field were not available across a broad geographical range and the two indices have an $c. 1 : 1$ relationship (Smith *et al.* 2007). The strength of the EIR data set is its broad geographical and temporal coverage (spanning the African continent from 1979 to 1996) and its methodological consistency.

To derive the mean temperature during the transmission season, we matched the length and timing of the transmission season with climate data from the ERA40 database. Because the MARA database provided the length but not the start and end months of the transmission season, we derived the transmission season using the MARA georeferenced start-of-season and the end-of-season maps (Fig. S3), combined with the length of transmission season data from the MARA database. When there were discrepancies in the length of transmission season derived from the maps vs. the MARA database, we assumed that the database was correct. We then used the derived start and end dates of the transmission season to extract a time series of the temperature and rainfall characteristics for each site from the ERA40 database. We aggregated the climate data to the monthly time-step and selected the one-degree grid cells that were associated with the field study locations. We did not include study locations that mapped into the 'no transmission' category or that lacked length of transmission season information, resulting in a loss of 50 (of 193) sites recorded in the database.

Rainfall is also important for malaria transmission. For this reason, we excluded locations that were too dry for transmission. We initially included rainfall as a covariate in our analysis, but it explained little additional variance, probably because rainfall sufficiently exceeded the threshold for transmission at all sites (the uncorrected data are plotted). Although mean transmission season temperature is an imperfect measure, it is the best available data with which to test the predictions of our model. We did not include temperature variation in the plot of EIR because our goal was to evaluate the model fit to mean temperature. Some of the unexplained variations in the relationship between transmission and mean temperature may be due to temperature variation; if we were attempting to explain variation in EIR, including temperature variation potentially would have been important. Nonetheless, because the R_0 curve is nearly symmetrical, temperature fluctuation would likely have little effect on the optimal mean temperature for transmission (Paaijmans, K.P., Ben-Horin, T., Lafferty, K.D., Johnson, L.R., McNally, A., Mordecai, E.A., Pawar, S., Ryan, S.J. & Thomas, M.B., in preparation).

To check that our temperature estimates from the ERA40 database were accurate, we compared them with the values for mean temperature during the transmission season listed in the original articles from the MARA database. Overall, our estimates were accurate. Of the 17 articles that provided temperature data, 15 had mean transmission-season temperatures within 1 °C of our estimate (corresponding to 36 of the 39 EIR data points we verified). For the three data points in which our temperature estimates did not match those in the article, we used the mean transmission-season temperatures listed in the ori-

ginal articles. While the remaining 43 articles did not provide transmission-season temperature information, the ERA40 temperature estimates are just as likely to be accurate for these studies.

We assumed that temperature would have the strongest impact on transmission in the sites with the highest EIR within areas of similar temperature, implying that malaria was most difficult to control in these locations. To visualise this relationship, we highlighted the maximum EIR within each bin of 10 consecutive data points ordered by temperature (maxima are the filled circles in Fig. 2). Bin size did not strongly affect the results: maximum EIR always occurred around 25–26 °C (Fig. S1). We overlaid the new and previous R_0 curves on the same figure for ease of comparison.

Parameter sensitivity

We determined the effect of each life-history parameter on the temperature peak for R_0 by performing a sensitivity analysis (Fig. 3a). We calculated the additive contribution of the temperature sensitivity of each parameter to the overall sensitivity of R_0 (see Appendix S1 for equations). Because mosquito mortality rate had the strongest effect on the thermal response of R_0 , we examined the sensitivity of R_0 to error in the mortality thermal response. We calculated 95%

simultaneous prediction bounds P_μ (Seber & Wild 2003) for the fitted μ (mortality rate) model, which are given by

$$P_i = \hat{y} \pm f \sqrt{x S x'}$$

where \hat{y} is the fitted value for temperature value x , f is calculated from the F distribution at $\alpha = 0.05$, and S is the covariance matrix of the coefficient estimates obtained from the OLS fitting. These prediction bounds measure the confidence that a new observation lies within the interval regardless of the predictor value. Thus, calculating R_0 at the upper and lower prediction bounds indicates the robustness of the location of the peak and width of the thermal-dependence curve to variation in the mortality function (Fig. 3b).

We also plotted R_0 vs. T curves in which each parameter is held constant with respect to temperature to visualise the effect of each parameter on the temperature sensitivity of R_0 (Fig. 3c). Doing so also allows us to indirectly test sensitivity of our results to variation in thermal-response parameters (such as T_{pk}) that may differ across mosquito species and geographical location.

RESULTS

All mosquito and parasite trait–temperature relationships were unimodal (Fig. 1, Tables 1 and S2). In contrast to the assumptions of

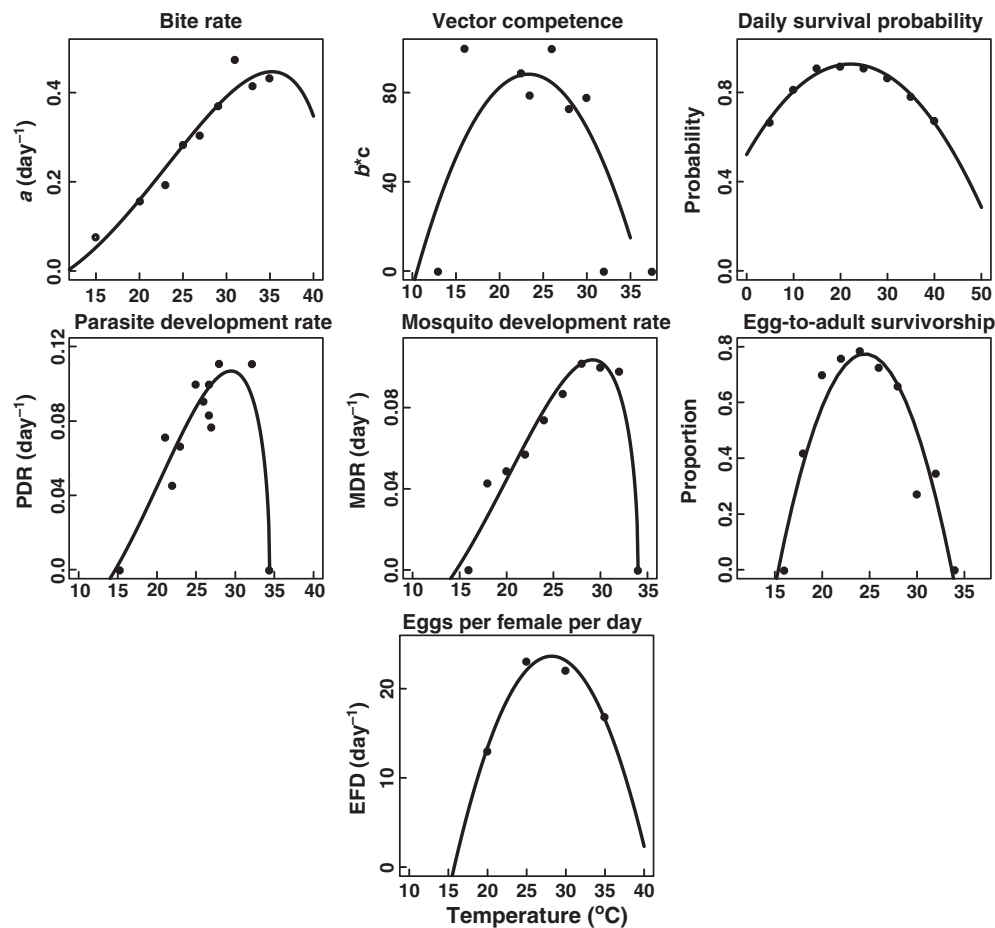


Figure 1 Thermal performance curves for all mosquito and parasite life-history traits that together determine R_0 . Note that the temperature ranges (x -axes) differ for different traits. Data sources, parameter descriptions and fit functions are listed in Table 2. The original mortality data are shown in Fig. S2.

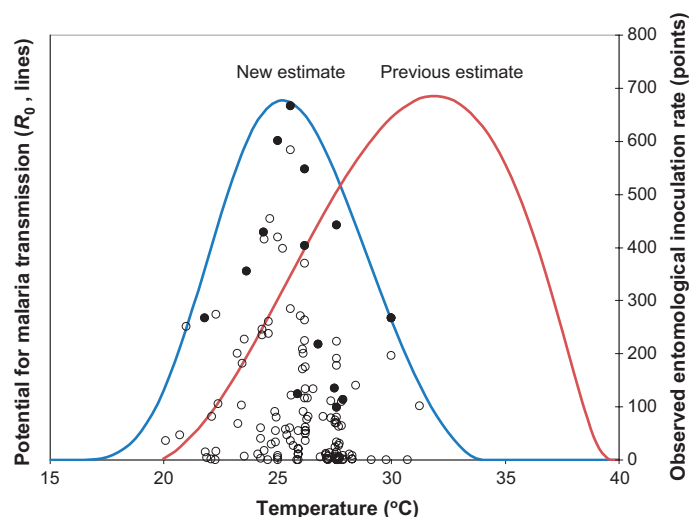


Figure 2 Temperature dependence of malaria risk. The blue curve is our estimate ('new estimate'), whereas the red curve ('previous estimate') uses the temperature-dependence assumptions from the Parham & Michael (2010) model. The points are the published entomological inoculation rate (EIR) data from Africa, plotted against the mean temperature during transmission season ($n = 122$). The y -axis for R_0 is not scaled because its absolute value depends on other climatic and socio-economic factors. Filled circles represent the maximum EIR within each bin of 10 sequential temperature points; the open circles demarcate the remaining data points. We highlight the maximum EIR in each bin because it represents the location where malaria is most difficult to control, and most likely to be influenced by temperature.

previous models (Table 1), all parameters were thermally constrained at both low and high temperatures, and unimodal curves [i.e. quadratic or Briere (Briere *et al.* 1999); see Materials and Methods] fit the data better than linear relationships (Table S1). Biting rate (the inverse of gonotrophic cycle length) was not measured above 34 °C, making the upper thermal limit more ambiguous than for the other measures. Still, the Briere curve was the best fit to biting rate (Table S1), which declined slightly above 30 °C.

Incorporating these unimodal curves into a model of R_0 predicts that the optimal temperature for malaria transmission is 25 °C, with transmission occurring between 16 °C (CT_{min}) and 34 °C (CT_{max} ; Fig. 2). This predicted optimum is 5–7 °C cooler than previous estimates from models that assumed linear or constant relationships between life-history parameters and temperature (Table 1). The predicted optimum temperature for malaria transmission, which depends heavily on mosquito physiology, matches the optimal temperature of 24.7 ± 0.48 °C for population growth measured for eight other Diptera species (Huey & Berrigan 2001).

The response of observed transmission potential (EIR) to local mean temperature during the transmission season in Africa was consistent with model predictions. The highest observed EIR values were recorded when mean transmission season temperature ranged from 24 to 26 °C (Fig. 2, Fig. S1), and transmission potential declined steeply below 20 °C and above 28 °C. This matches the predicted temperature optimum and range for malaria risk from the model. The variability among data points with similar mean temperatures reflects the influence of other climate and socio-economic factors, including vector control, on malaria transmission.

We examined the sensitivity of malaria transmission to each of its component life-history parameters by performing a sensitivity analy-

sis on the fully parameterised R_0 model (Fig. 3a). The figure depicts the effect of each parameter on the temperature sensitivity of R_0 , with each line crossing the x -axis at that parameter's temperature peak. Adult mosquito mortality, μ , had the strongest effect on the temperature sensitivity of R_0 , first because it enters both the original R_0 equation (1) and the mosquito density equation (Appendix eqn 5), resulting in a μ^{-3} term in the final model (2), and second because its peak of 22.1 °C is several degrees lower than the peaks of most other parameters. Nonetheless, shifting μ to its upper and lower prediction bounds shifted the temperature peak for transmission by < 1 °C (Fig. 3b). Even under the extreme assumption that mosquito survival was constant across temperature, the optimum transmission temperature only increased by ≈ 3 °C, still 2–4 °C lower than current model estimates (Table 1, Fig. 3c). This indicates that although mosquito mortality lowers the thermal optimum for malaria transmission, the 6 °C difference between previous models and ours is driven by the combined effect of all life-history parameters, and not by mortality alone. In addition, the model predictions were not sensitive to the other life-history parameters, indicating that any error in individual thermal responses resulting from the use of mosquito species other than African *Anopheles* species, or our choice of functional form (Briere or quadratic), was unlikely to affect our overall result (Fig. 3).

DISCUSSION

Consistent with a large body of thermal physiology work (Angilletta 2009; Dell *et al.* 2011), all of the mosquito and parasite life-history traits we examined peaked at intermediate temperatures well within the range experienced in nature (Fig. 1, Table 2). Ours is the first mechanistic model of malaria transmission to include empirically derived unimodal thermal responses for all mosquito and parasite traits involved in transmission. Combining the thermal responses that are constrained at both high and low temperatures limits malaria transmission (R_0) to temperatures between 16 and 34 °C with a peak at 25 °C. This new temperature optimum is 6 °C lower than estimates from previous mechanistic models (Martens *et al.* 1997; Craig *et al.* 1999; Parham & Michael 2010; Fig. 2, Table 1). For comparison, this difference in predicted optimal temperature is equivalent to a century of temperature change projected by the worst-case climate change scenarios [A1FI economic growth, fossil fuel intensive (Solomon *et al.* 2007)].

Our results help to explain earlier results from observational studies showing that malaria transmission often peaks in the autumn rather than summer, that temperatures above 30 °C may be detrimental to parasite development, and that mean monthly temperatures are 25 °C or above during the hottest month in tropical and equatorial zones, where transmission is greatest (Gill 1938; Pampana 1963). Because high temperatures often coincide with periods of low humidity in the tropics, it is difficult to discern the impact of temperature vs. humidity using observational models alone (Gill 1938). Early work attributed low transmission during the summer to low humidity, rather than high temperatures (Gill 1938), but our mechanistic model suggests temperature alone could suffice as an explanation.

One possible reason for the prior lack of biologically realistic thermal-response models is the scarcity of data relating *Anopheles* vital rates to temperature. Although many studies measure mosquito and parasite vital rates at a single temperature or in the field, few studies measure vital rates across a range of constant temperatures.

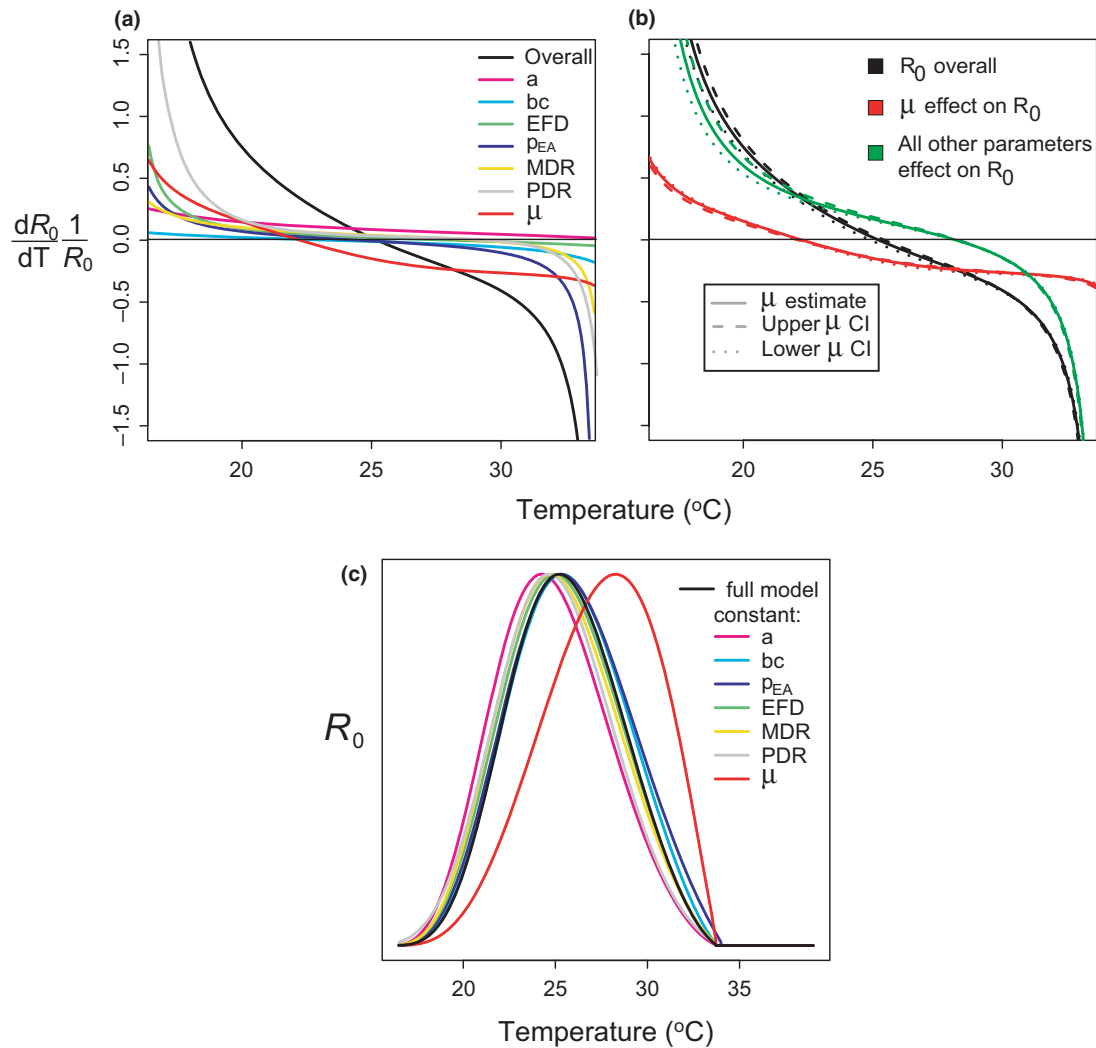


Figure 3 Sensitivity analysis. (a) The relative sensitivity of R_0 to each vital rate. Black curve: the derivative of R_0 with respect to temperature, per unit R_0 . Coloured curves: the effect of each parameter on the temperature sensitivity of R_0 (i.e. $dR_0/R_0 dx/dT$). (b) The effect of the adult mosquito mortality on the temperature sensitivity of R_0 . The red and green lines are, respectively, the effect of mortality and the combined effects of all other parameters on the temperature sensitivity of R_0 ; the black lines are the overall relative sensitivity of R_0 to temperature ($dR_0/R_0 dT$). Dashed lines represent the upper and lower 95% confidence intervals respectively. (c) The effect on R_0 of holding each parameter constant with respect to temperature.

In particular, no estimates for *Anopheles* fecundity at a range of controlled temperatures were available – clearly a much-needed avenue for future study. Nonetheless, sensitivity analysis suggests that our model predictions would not change substantially with additional data. The predicted relationship between malaria risk and temperature is robust to variation in temperature sensitivity of the various organismal traits. Although adult mosquito mortality has the largest effect on the temperature sensitivity of transmission, mortality alone cannot explain the 6 $^{\circ}\text{C}$ difference between the new optimal temperature estimate and previous estimates (Table 1).

Recent work has emphasised the importance of daily temperature variation in driving malaria transmission (Paaijmans *et al.* 2009, 2010). The rate summation approach applied in Paaijmans *et al.* (2009) only works using thermal performance curves based on constant temperatures: a basic thermal-response model such as ours is required for understanding the influence of temperature in a variable world (Paaijmans *et al.* 2009; Bozinovic *et al.* 2011). One application of our model is to integrate it over a range of temperature

means and daily ranges to understand the influence of daily temperature variation on malaria transmission; this is the subject of ongoing research.

Our approach of incorporating empirically validated temperature-response curves for all organismal traits that govern transmission could be applied for a range of infectious diseases, especially vector-borne diseases. The predicted optimal transmission temperature of 31 $^{\circ}\text{C}$ from previous models (Table 1) is inconsistent with the observation that locations with mean transmission season temperatures above 28 $^{\circ}\text{C}$ had very low transmission potential (EIR; Fig. 2), (Pampana 1963; Ikemoto 2008). By contrast, our model predictions indicate that temperate regions are suitable for transmission. This is consistent with historical records of malaria incidence (Hay *et al.* 2004) and suggests that economic development and vector control, not temperature, currently impede transmission in temperate climates (Lafferty 2009; Gething *et al.* 2010; Béguin *et al.* 2011). Nonetheless, vector control may become more challenging if climate change pushes temperatures closer to the 25 $^{\circ}\text{C}$ optimum.

The role of temperature in driving malaria transmission has been debated (Gething *et al.* 2010), in part because field data often confound the causative role of temperature with other climatic, geographical and socio-economic factors. In addition, these other climatic and societal factors can overwhelm the influence of temperature in some places (Gething *et al.* 2010). Our approach ensures that temperature is a driver and not a covariate by using thermal performance data measured at invariant temperatures, isolating the effects of temperature mean from variability. Although economic, demographic and direct control measures can outweigh the influence of temperature in some areas (Gething *et al.* 2010), it is clear that the strongest effects of temperature will occur in the locations where malaria is most difficult to control – the poorest and most vulnerable regions (Béguin *et al.* 2011).

Understanding the unimodal influence of temperature on malaria transmission will contribute to more accurate predictions about how climate change will affect malaria risk. R_0 is also a guiding tool for allocating disease control efforts effectively. Our model mechanistically links R_0 , thermal physiology models, and empirical data from *Anopheles* mosquitoes and *P. falciparum* parasites, and it agrees well with independently published field data. The model suggests that vector control will likely become more important, difficult and expensive in temperate areas as temperatures increase, but that some warm areas may simply become too hot to support malaria. This second conclusion is in contrast to previous models that predicted an optimum of 31 °C, which suggest that warming would increase malaria risk nearly everywhere (Table 1, but see Ikemoto 2008; Lafferty 2009). Our results further suggest that near their temperature limits, mosquitoes may seek more moderate microclimates, such as wells in tropical climates and human habitations in temperate zones. This model is not sufficient to predict malaria risk from mean temperatures in the field because variable temperature regimes that occur in nature might considerably alter transmission (Paaijmans *et al.* 2009; we intend to consider variability in future work). Quantitative predictions will additionally require global geographical data on current malaria burden, temperature, precipitation and land cover, and are clearly a much-needed topic for future research.

ACKNOWLEDGEMENTS

Andrew Read, Andrew Dobson, Jonathan Levine provided helpful comments on the manuscript. This work was conducted as a part of the Malaria and Climate Change Working Group supported by the Luce Environmental Science to Solutions Fellowship and the National Center for Ecological Analysis and Synthesis, a Center funded by NSF (Grant #EF-0553768), the University of California, Santa Barbara and the State of California. K.P.P. is funded by an NSF-EID programme grant (EF-0914384). C.B. was funded by NSF-GRF (DGE-1144085). E.d.M. is funded by an NSF Graduate Research Fellowship. T.B.H. is supported by a fellowship from the Michael J. Connell Trust. Any use of trade, product or firm names in this publication is for descriptive purposes only and does not imply endorsement by the US government.

AUTHOR CONTRIBUTIONS

EAM, KDL and KPP designed research; EdM, AM, SJR, TBH, EAM, KPP and TCS collected the data; LRJ, CB, KDL and SP performed the analysis; all authors wrote the paper.

REFERENCES

- Afrane, Y.A., Zhou, G., Lawson, B.W., Githeko, A.K. & Yan, G. (2007). Life-table analysis of *Anopheles arabiensis* in Western Kenya highland effects of land covers on larval and adult survivorship. *Am. J. Trop. Med. Hyg.*, *77*, 660–666.
- Alonso, D., Bouma, M.J. & Pascual, M. (2011). Epidemic malaria and warmer temperatures in recent decades in an East African highland. *Proc. R. Soc. Lond. B Biol. Sci.*, *278*, 1661–1669.
- Amarasekare, P. & Savage, V. (2012). A framework for elucidating the temperature dependence of fitness. *Am. Nat.*, *179*, 178–191.
- Angilletta, M.J. (2009). *Thermal Adaptation: A Theoretical and Empirical Synthesis*. Oxford University Press, New York.
- Bodker, R., Akida, J., Shayo, D., Kisinza, W., Msangeni, H.A. & Pedersen, E.M., *et al.* (2003). Relationship between altitude and intensity of malaria transmission in the Usambara Mountains, Tanzania. *J. Med. Entomol.*, *40*, 706–717.
- Bayoh, M.N. (2001). Studies on the development and survival of *Anopheles gambiae* sensu stricto at various temperatures and relative humidities. (PhD thesis). University of Durham, Durham, 134 pp.
- Bayoh, M.N. & Lindsay, S.W. (2003). Effect of temperature on the development of the aquatic stages of *Anopheles gambiae* sensu stricto (Diptera: Culicidae). *Bull. Entomol. Res.*, *93*, 375–381.
- Béguin, A., Hales, S., Rocklöv, J., Åström, C., Louis, V.R. & Sauerborn, R. (2011). The opposing effects of climate change and socio-economic development on the global distribution of malaria. *Glob. Environ. Change*, *21*, 1209–1214.
- Borland, I. (2001–2010). DigitizeIt 1.5.8b. In. DigitizeIt.
- Boyd, M.F. & Stratman-Thomas, W.K. (1933). A note on the transmission of quartan malaria by *Anopheles quadrimaculatus*. *Am. J. Trop. Med. Hyg.*, *13*, 265–271.
- Bozinovic, F., Bastias, D.A., Boher, F., Clavijo-Baquet, S., Estay, S.A. & Angilletta, M.J. Jr (2011). The mean and variance of environmental temperature interact to determine physiological tolerance and fitness. *Physiol. Biochem. Zool.*, *84*, 543–552.
- Briere, J.F., Pracros, P., Le Roux, A.Y. & Pierre, J.S. (1999). A novel rate model of temperature-dependent development for arthropods. *Environ. Entomol.*, *28*, 22–29.
- Craig, M.H., Snow, R.W. & leSueur, D. (1999). A climate-based distribution model of malaria transmission in sub-Saharan Africa. *Parasitol. Today*, *15*, 105–111.
- Delatte, H., Gimonneau, G., Triboire, A. & Fontenille, D. (2009). Influence of temperature on immature development, survival, longevity, fecundity, and gonotrophic cycles of *Aedes albopictus*, vector of chikungunya and dengue in the Indian Ocean. *J. Med. Entomol.*, *46*, 33–41.
- Dell, A.L., Pawar, S. & Savage, V.M. (2011). Systematic variation in the temperature dependence of physiological and ecological traits. *Proc. Natl Acad. Sci. USA*, *108*, 10591–10596.
- Deutsch, C.A., Tewksbury, J.J., Huey, R.B., Sheldon, K.S., Ghalambor, C.K., Haak, D.C. *et al.* (2008). Impacts of climate warming on terrestrial ectotherms across latitude. *Proc. Natl Acad. Sci. USA*, *105*, 6668–6672.
- Dietz, K. (1993). The estimation of the basic reproduction number for infectious diseases. *Stat. Methods Med. Res.*, *2*, 23–41.
- Eling, W., Hooghof, J., van de Vegte-Bolmer, M., Sauerwein, R. & van Gemert, G.-J. (2001). Tropical temperatures can inhibit development of the human malaria parasite *Plasmodium falciparum* in the mosquito. *Proc. Exp. Appl. Entomol.*, *12*, 151–156.
- Englund, G., Öhlund, G., Hein, C.L. & Diehl, S. (2011). Temperature dependence of the functional response. *Ecol. Lett.*, *14*, 914–921.
- Ermert, V., Fink, A.H., Jones, A.E. & Morse, A.P. (2011). Development of a new version of the Liverpool Malaria Model. I. Refining the parameter settings and mathematical formulation of basic processes based on a literature review. *Malar. J.*, *10*, 17.
- Gething, P.W., Smith, D.L., Patil, A.P., Tatem, A.J., Snow, R.W. & Hay, S.I. (2010). Climate change and the global malaria recession. *Nature*, *465*, 342–345.
- Gething, P., Van Boeckel, T., Smith, D., Guerra, C., Patil, A., Snow, R. *et al.* (2011). Modelling the global constraints of temperature on transmission of *Plasmodium falciparum* and *P. vivax*. *Parasit. Vectors*, *4*, 92.

- Gill, C.A. (1938). *The Seasonal Periodicity of Malaria and the Mechanism of the Epidemic Wave*. Churchill, Ltd, London.
- Hay, S.I., Rogers, D.J., Toomer, J.F. & Snow, R.W. (2000). Annual *Plasmodium falciparum* entomological inoculation rates (EIR) across Africa: literature survey, internet access and review. *Trans. R. Soc. Trop. Med. Hyg.*, 94, 113–127.
- Hay, S.I., Guerra, C.A., Tatem, A.J., Noor, A.M. & Snow, R.W. (2004). The global distribution and population at risk of malaria: past, present and future. *Lancet Infect. Dis.*, 4, 327–336.
- Hoshen, M.B. & Morse, A.P. (2005). A model structure for estimating malaria risk. In: *Environmental change and malaria risk: global and local implications* (eds. Takken, W. & Bogers, R.J.). Springer, Dordrecht, pp. 41–50.
- Huey, R.B. & Berrigan, D. (2001). Temperature, demography, and ectotherm fitness. *Am. Nat.*, 158, 204–210.
- Ikemoto, T. (2008). Tropical malaria does not mean hot environments. *J. Med. Entomol.*, 45, 963–969.
- Johnson, F.M., Eyring, H. & Stover, B.J. (1974). *The Theory of Rate Processes in Biology and Medicine*. John Wiley, New York.
- Knowles, R. & Basu, B.C. (1943). Laboratory studies on the infectivity of *Anopheles stephensi*. *J. Mal. Inst. India*, 5, 1–29.
- Lafferty, K.D. (2009). The ecology of climate change and infectious diseases. *Ecology*, 90, 888–900.
- Lardeux, F.J., Tejerina, R.H., Quispe, V. & Chavez, T.K. (2008). A physiological time analysis of the duration of the gonotrophic cycle of *Anopheles pseudopunctipennis* and its implications for malaria transmission in Bolivia. *Malar. J.*, 7, 17.
- Lyimo, E.O., Takken, W. & Koella, J.C. (1992). Effect of rearing temperature and larval density on larval survival, age at pupation and adult size of *Anopheles gambiae*. *Entomol. Exp. Appl.*, 63, 265–271.
- Martens, W.J.M., Jetten, T.H. & Focks, D.A. (1997). Sensitivity of malaria, schistosomiasis and dengue to global warming. *Clim. Chang.*, 35, 145–156.
- Neuheimer, A.B., Thresher, R.E., Lyle, J.M. & Semmens, J.M. (2011). Tolerance limit for fish growth exceeded by warming waters. *Nat. Clim. Chang.*, 1, 110–113.
- Paaijmans, K.P., Read, A.F. & Thomas, M.B. (2009). Understanding the link between malaria risk and climate. *Proc. Natl Acad. Sci. USA*, 106, 13844–13849.
- Paaijmans, K.P., Blanford, S., Bell, A.S., Blanford, J.I., Read, A.F. & Thomas, M. B. (2010). Influence of climate on malaria transmission depends on daily temperature variation. *Proc. Natl Acad. Sci. USA*, 107, 15135–15139.
- Pampuna, E. (1963). *A Textbook of Malaria Eradication*. Oxford University Press, London.
- Parham, P.E. & Michael, E. (2010). Modeling the effects of weather and climate change on malaria transmission. *Environ. Health Perspect.*, 118, 620–626.
- Pascual, M., Dobson, A.P. & Bouma, M.J. (2009). Underestimating malaria risk under variable temperatures. *Proc. Natl Acad. Sci. USA*, 106, 13645–13646.
- R Core Development Team. (2010). *R: A language and environment for statistical computing*. R Foundation for Statistical Computing, Vienna, Austria.
- Rogers, D.J. & Randolph, S.E. (2006). Climate change and vector-borne diseases. In: *Global Mapping of Infectious Diseases: Methods, Examples and Emerging Applications (Advances in Parasitology)* (eds Hay, S.I., Graham, A. & Rogers, D.J.). Elsevier, San Diego, CA, pp. 345–381.
- Seber, G.A.F. & Wild, C.J. (2003). *Nonlinear Regression*. Wiley-Interscience, Hoboken, NJ.
- Shute, P.G. & Maryon, M. (1952). A study of human malaria oocysts as an aid to species diagnosis. *Trans. R. Soc. Trop. Med. Hyg.*, 46, 275–292.
- Siddons, L.B. (1944). Observations on the influence of atmospheric temperature and humidity on the infectivity of *Anopheles culicifacies giles*. *J. Mal. Inst. India*, 5, 375–388.
- Smith, D.L., McKenzie, F.E., Snow, R.W. & Hay, S.I. (2007). Revisiting the basic reproductive number for malaria and its implications for malaria control. *PLoS Biol.*, 5, e42.
- Solomon, S., Hegerl, G., Heimann, M., Hewitson, B., Hoskins, B., Joos, F. et al. (2007). Technical Summary. In: *Climate Change 2007: The Physical Science Basis. Contribution of Working Group 1 to the Fourth Assessment Report of the Intergovernmental Panel on Climate Change*. (eds. Solomon, S., Qin, D., Manning, M., Chen, Z., Marquis, M., Averyt, K.B., Tignor, M., Miller, H.L.). Cambridge University Press, New York, pp. 19–91.
- Stratman-Thomas, W.K. (1940). The influence of temperature on *Plasmodium vivax*. *Am. J. Trop. Med. Hyg.*, 20, 703–715.
- Takken, W., Klowden, M.J. & Chambers, G.M. (1998). Effect of body size on host seeking and blood meal utilization in *Anopheles gambiae sensu stricto* (Diptera: Culicidae): the disadvantage of being small. *J. Med. Entomol.*, 35, 639–645.
- Takken, W., Stuke, K. & Klowden, M.J. (2002). Biological differences in reproductive strategy between the mosquito sibling species *Anopheles gambiae sensu stricto* and *An. quadrimaculatus*. *Entomol. Exp. Appl.*, 103, 83–89.
- Uppala, S.M., Källberg, P.W., Simmons, A.J., Andrae, U., da Costa Bechtold, V., Fiorino, M. et al. (2005). The ERA-40 re-analysis. *Q. J. R. Meteorol. Soc.*, 131, 2961–3012.
- Vaughan, J.A., Noden, B.H. & Beier, J.C. (1992). Population dynamics of *Plasmodium falciparum* sporogony in laboratory-infected *Anopheles gambiae*. *J. Parasitol.*, 78, 716–724.
- WHO (2011). *World Malaria Report 2011*. World Health Organization, Geneva, p. 278.

SUPPORTING INFORMATION

Additional Supporting Information may be downloaded via the online version of this article at Wiley Online Library (www.ecologyletters.com).

As a service to our authors and readers, this journal provides supporting information supplied by the authors. Such materials are peer-reviewed and may be re-organised for online delivery, but are not copy-edited or typeset. Technical support issues arising from supporting information (other than missing files) should be addressed to the authors.

Editor, Peter Thrall

Manuscript received 30 April 2012

First decision made 11 June 2012

Second decision made 5 September 2012

Manuscript accepted 11 September 2012